

# The Rankine Vortex Model

By DARIO B. GIAIOTTI<sup>1</sup>† AND FULVIO STEL<sup>1</sup>

<sup>1</sup>Regional Meteorological Observatory, via Oberdan, 16/A I-33040 Visco (UD), ITALY

(4 October 2006)

The Rankine vortex model is a circular flow in which an inner circular region about the origin is in solid rotation, while the outer region is free of vorticity, the speed being inversely proportional to the distance from the origin. This flow model has occasionally been used for the wind distribution in a hurricane and in a tornado.

---

## 1. Definition of the Rankine vortex.

The Rankine vortex is a fluid flow having radial symmetry. Its definition is natural in a cylindrical coordinate system  $(r, \theta, z)$ , where the symmetry axis is the  $z$  coordinate axis, the  $r$  axis and the  $\theta$  axis lie on the plane normal to the  $z$  axis as shown in figure 1.

The vortex has the velocity field always normal to both the symmetry axis  $z$  and the radial vector  $\mathbf{r}$ . This means that the velocity is parallel to the  $\mathbf{j}$  unit vector. The intensity of the flow, that is the velocity vector modulus, is a function of the radial distance only  $r$ . The inner part of the vortex is in solid rotation, then its modulus is proportional to  $r$ , while the outer part is inversely proportional to the radial distance  $r$ . The maximum intensity of the flow is reached at the characteristic distance of the vortex,  $R$ , where there is the change between the inner linear behavior and the external hyperbolic one. Analytically the Rankine vortex is defined as follow:

$$\mathbf{v} = v_r \mathbf{i} + v_\theta \mathbf{j} + v_z \mathbf{k} \text{ where } \begin{cases} v_r = 0 \\ v_\theta = \begin{cases} V_R \frac{r}{R} & \text{if } 0 \leq r < R \\ V_R \frac{R}{r} & \text{if } R \leq r \end{cases} \\ v_z = 0 \end{cases} \quad (1.1)$$

and  $V_R$  is the maximum flow intensity. The behavior of the  $v_\theta$  vector component is presented in figure 2.

† e-mail: dario.giaiotti@osmer.fvg.it

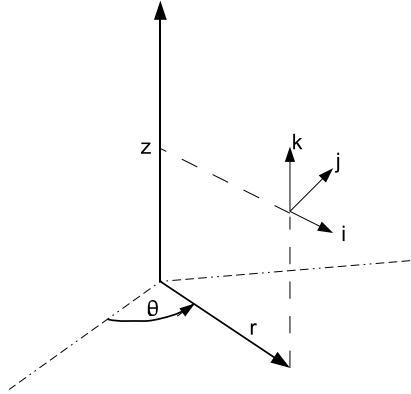


FIGURE 1. The cylindrical coordinate system adopted for the description of the Rankine vortex model. The unit normal vectors set  $(\mathbf{i}, \mathbf{j}, \mathbf{k})$  is reported in the point identified by coordinates  $(r, \theta, z)$ .

## 2. The vorticity field

One of the main features of the Rankine vortex is its vorticity field. In fact according to the definition of the vortex velocity field (1.1) and the application of the curl operator in cylindrical coordinates (A 4), it is evident that the vortex presents vertical vorticity component only. Furthermore the vorticity field modulus is constant in the inner part of the vortex, it is positive and it is a function of the maximum flow velocity and the vortex characteristic distance only. In the outer region of the vortex, the flow has no vorticity at all.

$$\nabla \times \mathbf{v} = \mathbf{k} \frac{1}{r} \frac{\partial(rv_\theta)}{\partial r} = \mathbf{k} \left( \frac{v_\theta}{r} + \frac{\partial v_\theta}{\partial r} \right) = \mathbf{k} \begin{cases} 2\frac{V_R}{R} & \text{if } 0 \leq r < R \\ 0 & \text{if } R \leq r \end{cases} \quad (2.1)$$

It is worth to note that the Rankine vortex is characterized by a continuous velocity field, but with a discontinuity in vorticity at the characteristic distance. This has relevant consequences on the turbulence in that region of the domain Batchelor (1993).

## 3. Applications of the model to atmospheric systems

The Rankine vortex is a simple model, but it can be considered suitable for the description of some typical atmospheric phenomena. Nowadays, thanks to the Doppler radar measurements, several cases of well organized convective cell, named mesocyclones, have been observed and the corresponding velocity fields have been measured. Mesocyclones can be approximated to cylindrical rotating convective structures having a inner core of

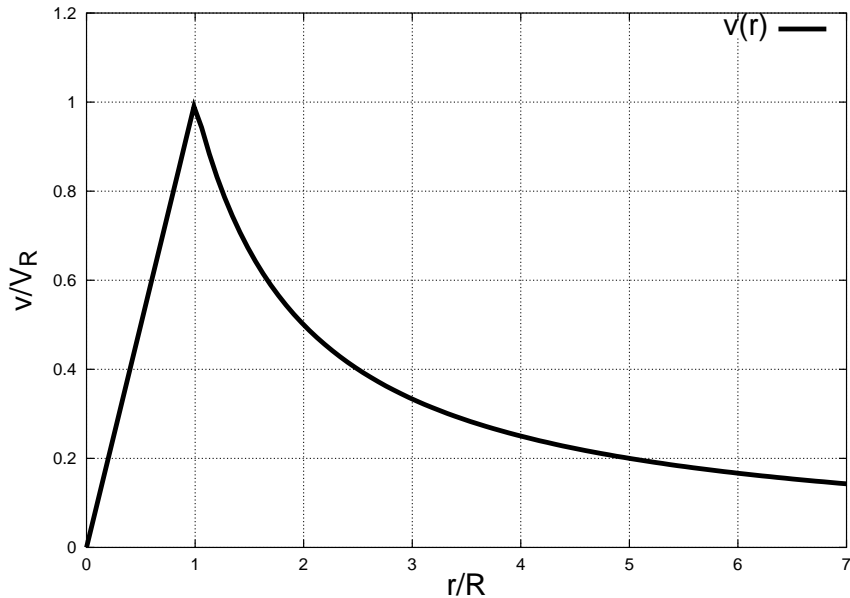


FIGURE 2. The Rankine vortex model is characterized by a flow that is always and everywhere parallel to the  $\mathbf{j}$  unit vector, so the only non null vector component is the  $v_\theta$  which is also the total velocity vector modulus. In this figure the normalized velocity vector modulus ( $v/V_R$ ) is plotted against the normalized radial distance ( $r/R$ ). Note that at the characteristic distance  $R$  there flow is continuous, but the flow regime changes, from a solid rotation for  $0 \leq r < R$  to a hyperbolic decrease at distances greater or equal than  $R$ .

about 5 km diameter that is in solid rotation and an outer rotating region in which the velocity drops with a law very close to the inverse of the distance. The peak velocity of the mesocyclone is reached at its characteristic distance, the external border of the inner core, and accounts of several meters per second, generally speeds larger than  $10 \text{ m s}^{-1}$  have been measured and very often more than  $20 \text{ m s}^{-1}$ , see Bertato *et al.* (2003) and Brown *et al.* (2005) as examples.

In figure 3 is reported the comparison between Doppler radar measurements, of a mesocyclone observed by means of the WSR-88D Doppler radar network, which is operating in the United States, and a Rankine model of the mesocyclone Brown *et al.* (2005).

Tornadoes, see figure 4, present the Rankine vortex structure, even if the vortex structure has a quick dynamics, evolving from the early no vortex stage to its end in a few minutes. The radial profile of the tangential, ( $v_\theta$ ) (azimuthal), wind component has been measured in several cases of tornado, by means of mobile Doppler radars and it shows the typical Rankine vortex model, see figure 5 Brown *et al.* (2005). Of course the tornado is characterized by a non null radial component of the wind ( $v_r$ ), especially at the

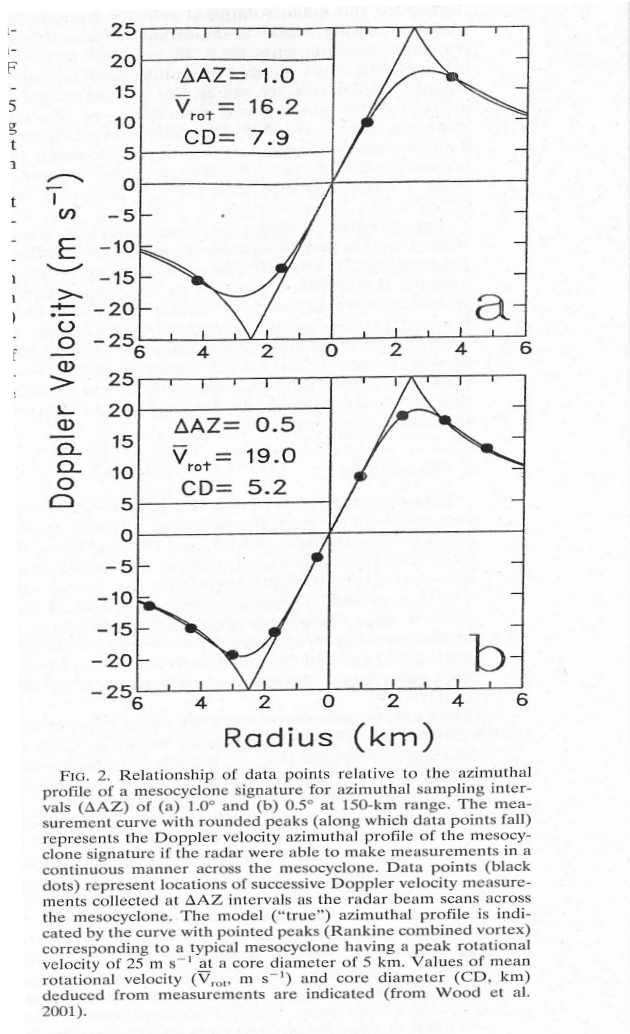


FIG. 2. Relationship of data points relative to the azimuthal profile of a mesocyclone signature for azimuthal sampling intervals ( $\Delta AZ$ ) of (a)  $1.0^\circ$  and (b)  $0.5^\circ$  at 150-km range. The measurement curve with rounded peaks (along which data points fall) represents the Doppler velocity azimuthal profile of the mesocyclone signature if the radar were able to make measurements in a continuous manner across the mesocyclone. Data points (black dots) represent locations of successive Doppler velocity measurements collected at  $\Delta AZ$  intervals as the radar beam scans across the mesocyclone. The model ("true") azimuthal profile is indicated by the curve with pointed peaks (Rankine combined vortex) corresponding to a typical mesocyclone having a peak rotational velocity of  $25 \text{ m s}^{-1}$  at a core diameter of 5 km. Values of mean rotational velocity ( $\bar{V}_{\text{rot}}$ ,  $\text{m s}^{-1}$ ) and core diameter (CD, km) deduced from measurements are indicated (from Wood et al. 2001).

FIGURE 3. Doppler radar measurements, of a mesocyclone observed by means of the WSR-88D Doppler radar network operating in the United States, and a Rankine model of the mesocyclone. Velocities in  $\text{ms}^{-1}$  are reported along the ordinate, while in abscissa there is the distance from the mesocyclone axis in  $\text{km}$ . Positive speeds represents radial velocities measured outward the radar, negative speeds are velocities toward the radar. Figure taken from the paper Brown *et al.* (2005). Measurements of Doppler mesocyclone velocity across the mesocyclonic structure are marked by solid black dots, while Rankine model profile is the solid curve with pointed peaks. The smoother curve passing through the measurement points represents a model of wind profile if the radar were able to measure in a continuous manner across the mesocyclone.

ground boundary. The radial component is usually an order of magnitude smaller than the tangential one, as shown in the sequence of measurements presented in the figure 6, where six snapshots of a tornado radial and azimuthal velocities have been taken about



FIGURE 4. Picture of the tornado whose measures are reported in figures 5 and 6. The tornado occurred in Bassett, Nebraska, on June 1999. Figure taken from the Bluestein *et al.* (2003) paper.

every 20 seconds. Positive radial wind values mean radial outflow, while negative ones correspond to radial inflow.

From those figures it is possible to note the increase of the azimuthal wind speed from the tornado center, qualitatively similar to the solid rotation part of the Rankine vortex, and the wind speed decrease after the characteristic distance. For this tornado, the characteristic distance ( $R$ ) is about  $0.2\text{ km}$ , as one can guess from figures 5 and 6 looking at the radial distance where the tangential velocity gets its maximum value. It is worth to note that the maximum tangential velocity is close to  $30\text{ m s}^{-1}$ . Information concerning the central part of the vortex, that is for  $r < 0.1\text{ km}$ , are not available because there were not enough scatterers allowing the radar signal to be significantly reflected backward to the receiver.

Even if qualitatively the Rankine vortex model fits the radial behavior of the tornado azimuthal velocity, quantitatively the deviation from the Rankine model is evident in the vorticity field as computed from the data, see figure 9. The time evolution of the vorticity vertical component, computed according to the third term of the right hand side of the formula A 4, does not characterize the tornado by a simply two regions constant field, that is the constant vorticity inner core and an outer null vorticity environment, separated by a discontinuity. As shown in the sequence of figure 9, the transition from the inner high

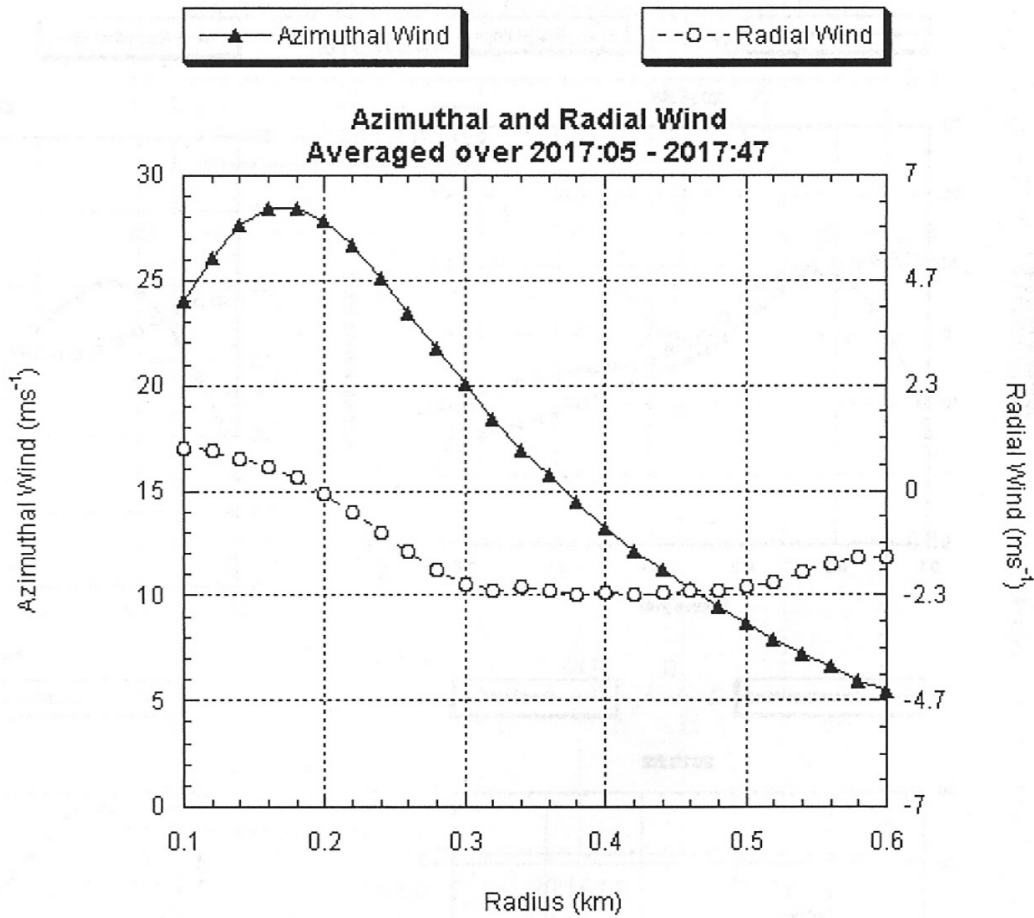


FIG. 5. As in Fig. 4, but for data averaged over the period from 2017:05 to 2017:47 CDT, when the tornado was most intense.

FIGURE 5. Averaged azimuthal and radial wind speeds over the most intense 40 seconds of the tornado existence. Azimuthal wind component measurements are plotted as filled triangles, connected with a solid line. Their scale, in  $ms^{-1}$  is reported on the left. Open circles connected with a dashed line report the radial component of the tornado velocity. The corresponding scale in  $ms^{-1}$  is on the right of the plot. Figure taken from the Bluestein *et al.* (2003) paper.

vorticity region,  $|\nabla \times \mathbf{v}| \simeq 0.3 s^{-1}$ , to the close to zero vorticity outer region is revealed by several measurement points and covers a space comparable with the inner vortex core  $R$ .

The smallest structures showing a Rankine vortex signature are the dust devils. These vortices take place in clear sky and fair weather conditions and usually they do not

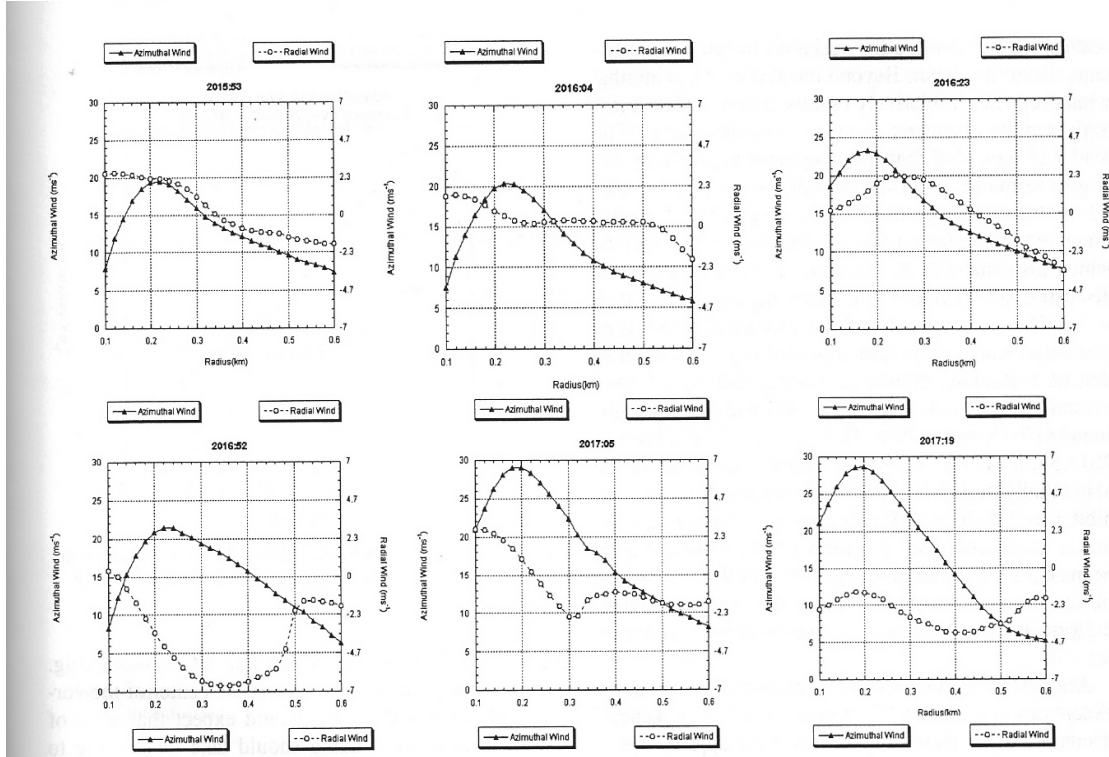


FIGURE 6. Azimuthal wind component measurements are reported by means of triangles connected with a solid line. Their scale, in  $ms^{-1}$  is reported on the left. Open circles connected with a dashed line report the radial component of the tornado velocity. The corresponding scale in  $ms^{-1}$  is reported on the right of the plots. In this sequence, each plot is a snapshot taken by the Doppler radar every about 20 seconds. Figures taken from the Bluestein *et al.* (2003) paper.

produce damages, because they produce wind speeds that only seldom reach  $10 ms^{-1}$ . Doppler radar measurement of dust devils (Bluestein & Weiss 2004) have shown that in some cases they behave like Rankine vortices, see figure 7, in other cases their cores are not in solid rotation, but the tangential wind component presents a more than linear decrease towards the vortex center, see figure 8. According to the measurement so far published in literature, the outer region of the dust devils is close to the null vorticity flow regime typical of the Rankine vortex model. In spite to the weaker wind velocity, dust devils have vorticity vertical component comparable to that measured in the tornadoes' core. From figures 7 and 8 it is easy to recognize that the two dust devils studied by Bluestein & Weiss (2004) reach peak vorticity larger than  $0.5 s^{-1}$ . The peaks are placed close to area of the tangential velocity maximum.

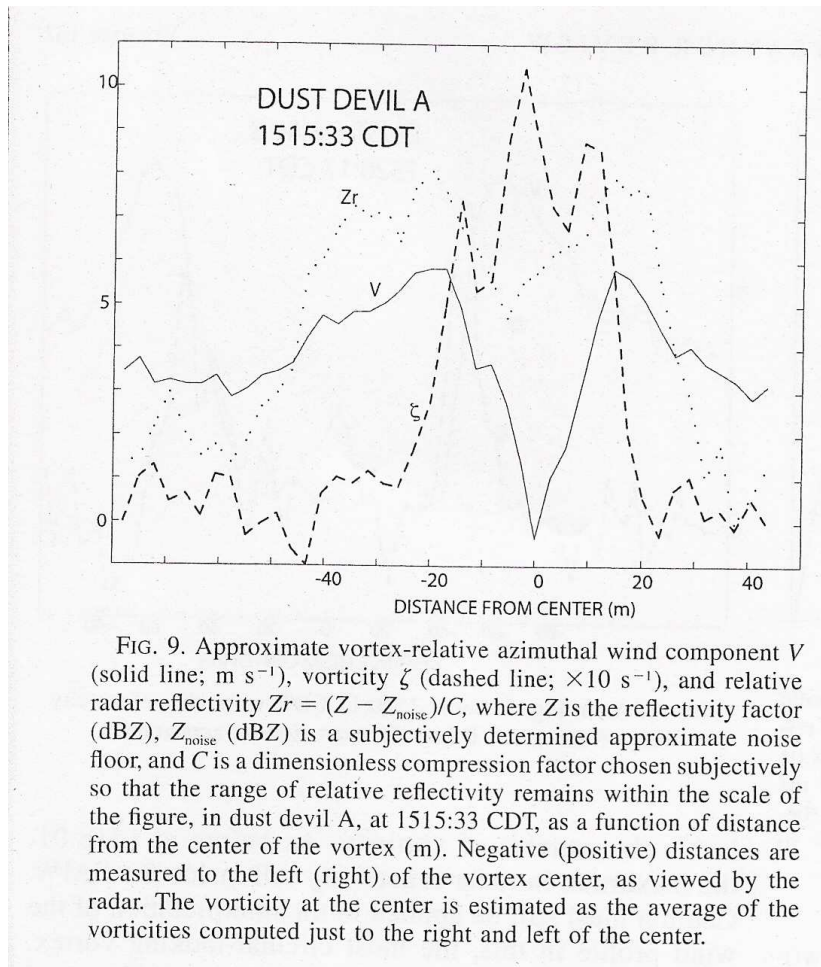


FIGURE 7. Radial profiles for a dust devil occurred in Texas on May 1999 and observed by means of a mobile Doppler radar. The solid black line reports the tangential velocity of the vortex in  $\text{m s}^{-1}$ . The vertical component of the vorticity is plotted in dashed line and it is expressed in units of  $\times 10 \text{ s}^{-1}$ . The dotted line represents the relative radar reflectivity; this variable is not relevant in the context of this lecture so it is not describe in this caption. Picture taken from the Bluestein & Weiss (2004) paper.

Take your notes here below



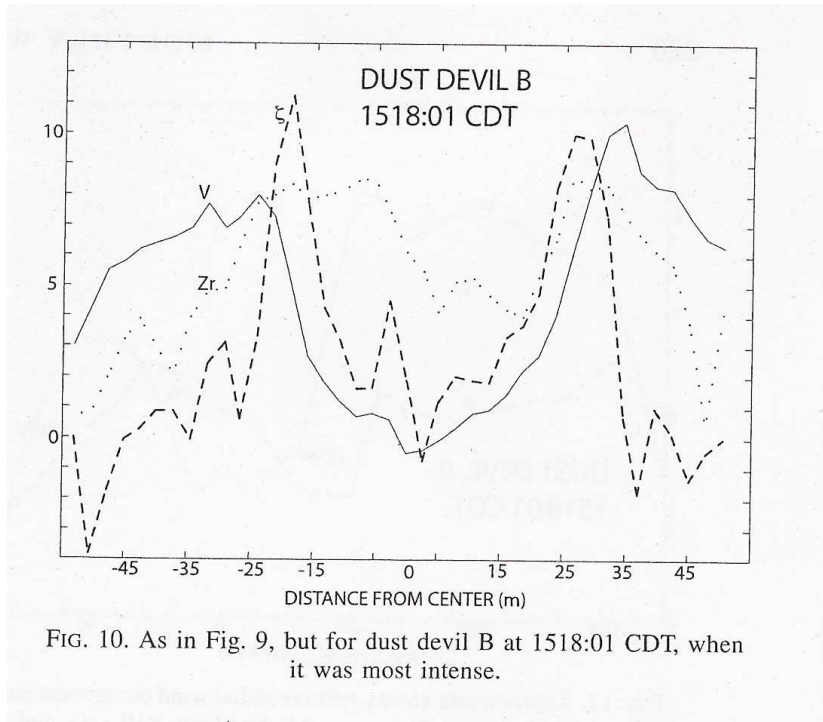


FIGURE 8. As in figure 7, but for another dust devil, which was observed in the same day of that presented in figure 7, but more intense. Picture taken from the Bluestein & Weiss (2004) paper.

Take your notes here below

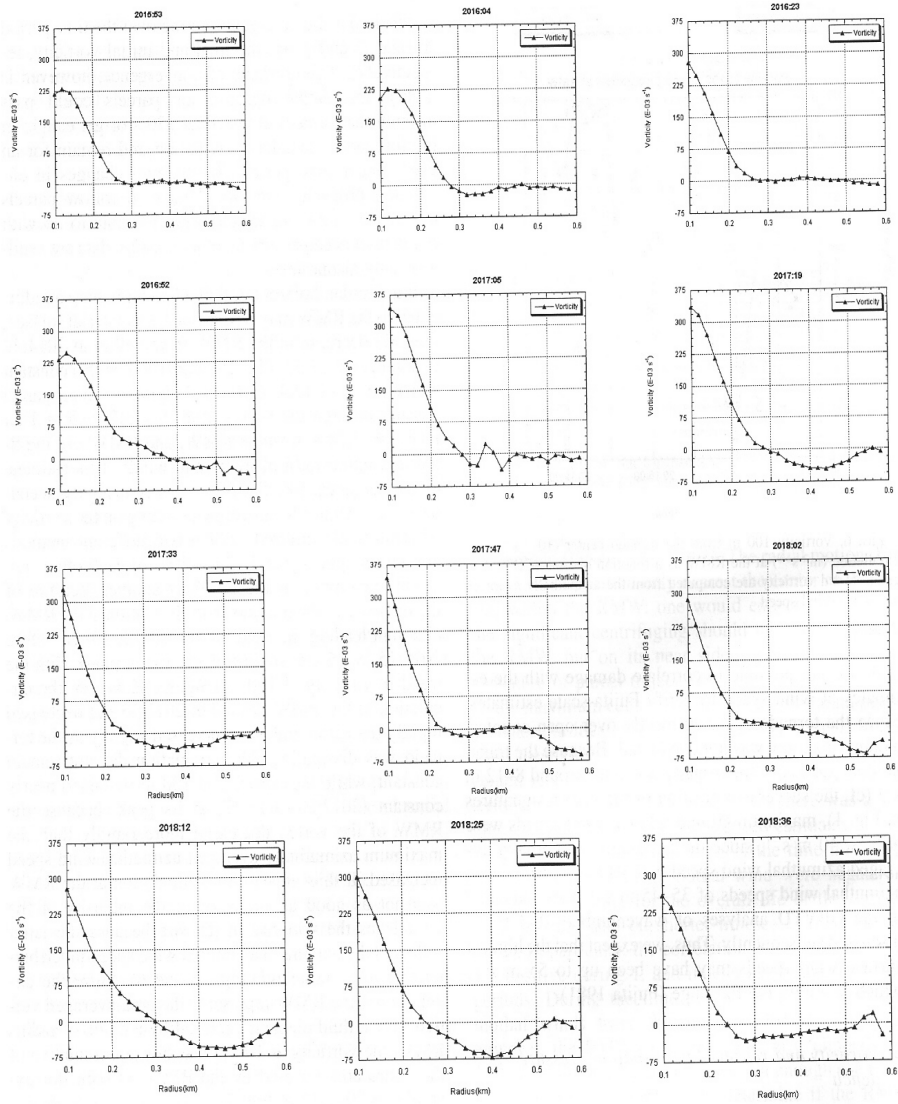


Fig. 7. Vorticity ( $10^{-3} \text{ s}^{-1}$ ) as a function of distance from the center of the tornado during the period from 2015:53 to 2018:36 CDT.

FIGURE 9. Time series of the vorticity vertical component for the June 1999 Bassett, Nebraska, tornado. The figures show the radial behavior of the vorticity, that was computed from the Doppler radar data according to the third term of the right hand side of the formula A 4, Vorticity is reported along the ordinate axis in  $10^{-3} \text{ s}^{-1}$  units, while the abscissa axis gives the distance from the tornado center in  $\text{km}$ .

Take your notes here below

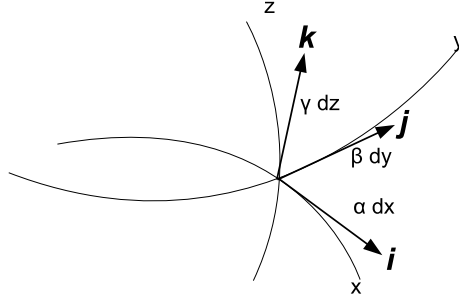


FIGURE 10. The general orthogonal curvilinear coordinate system. Unit vectors tangent to the coordinate lines ( $\mathbf{i}, \mathbf{j}, \mathbf{k}$ ) are normal to each other in every point of the space. The elementary displacements along coordinate lines are functions of the elementary coordinate displacements ( $dx, dy, dz$ ) and of the point where they are computed through the functions  $\alpha(x, y, z), \beta(x, y, z), \gamma(x, y, z)$ .

### Appendix A. The curl operator in cylindrical coordinates

Following the general expression for the curl operator in three-dimensional orthogonal curvilinear coordinates ( $x, y, z$ ), see figure 10, defined by means of the Euclidean metric as follow:

$$ds^2 = (\alpha dx)^2 + (\beta dy)^2 + (\gamma dz)^2 \quad (\text{A } 1)$$

the operator is defined by means of the determinant notation (Batchelor 1994, see Appendix 2):

$$\nabla \times \mathbf{F} = \frac{1}{\alpha\beta\gamma} \begin{vmatrix} \alpha\mathbf{i} & \beta\mathbf{j} & \gamma\mathbf{k} \\ \frac{\partial}{\partial x} & \frac{\partial}{\partial y} & \frac{\partial}{\partial z} \\ \alpha F_x & \beta F_y & \gamma F_z \end{vmatrix} \quad (\text{A } 2)$$

Applying this general result to the cylindrical coordinate system, see figure 1, which is characterized by (Batchelor 1994, see Appendix 2) and (Fogiel 2001, see Chalper 9)

$$\alpha = 1 \quad \beta = r \quad \gamma = 1 \quad (\text{A } 3)$$

then the curl components are as follow:

$$\nabla \times \mathbf{F} = \mathbf{i} \left[ \frac{1}{r} \left( \frac{\partial F_z}{\partial \theta} - \frac{\partial(rF_\theta)}{\partial z} \right) \right] + \mathbf{j} \left[ \frac{\partial F_r}{\partial z} - \frac{\partial F_z}{\partial r} \right] + \mathbf{k} \left[ \frac{1}{r} \left( \frac{\partial(rF_\theta)}{\partial r} - \frac{\partial F_r}{\partial \theta} \right) \right] \quad (\text{A } 4)$$

**Appendix B. Exercises***B.1. Exercise 1*

Consider the Rankine vortex model (1.1) and add to it a constant flow, then compute the vorticity field. Is the vorticity changed? Then consider a mesocyclone or a tornado at the mid latitudes which is described by a Rankine vortex model, add to it a synoptic flow and compute its potential vorticity. What about the vorticity of a tropical cyclone described by a Rankine vortex model and moving from the tropics to the mid latitudes? See (Crisciani 2005, cap. 7), Dutton (1995), Gill (1982), Holton (1972*a*), Pedlosky (1987).

*B.2. Exercise 2*

Consider the Rankine vortex model (1.1), compute and plot the trajectories for a set three fluid parcels having initial conditions:  $(0, 0, 0)$ ,  $(R/2, 0, 0)$  and  $(2R, 0, 0)$ . Then add to the Rankine vortex model a constant flow a recompute and plot the trajectories for the same three parcels.

*B.3. Exercise 3*

With reference to the figure 5, in particular using the maximum azimuthal velocity  $V_R$  and the corresponding characteristic vortex radius  $R$ , assume that the tornado is in cyclostrophic balance, Giaiotti & Stel (2005), Holton (1972*b*), at  $r = R$ , then compute the radial component of the pressure gradient in that point. Furthermore, assuming the Rankine vortex model, compute the overall pressure difference between the characteristic distance region and the center of the tornado. Use the  $V_R$  value deduced by figure 5 and assume that at  $r = R$  the atmospheric pressure is  $1013.0 \text{ hPa}$ .

**Appendix C. Historical notes***C.1. William John Macquorn Rankine*

Born: 1820 in Edinburgh, Great Britain.

Died: 1872 in Edinburgh, Great Britain.

William John Macquorn Rankine, a Scottish engineer and physicist, contributed significantly to the thermodynamics. Rankine developed a fully complete theory of the steam engine furthermore his interests were varied and in many branches of mathematics and engineering.

Rankine interpreted the results of his molecular theories in terms of energy and its transformation. That lead him to the energetics which gave an account of dynamics in terms of energy and transformation rather than force. Energetics offered Rankine an alternative approach, to his thermodynamics studies reducing the use of the molecular vortexes method he developed earlier. He considered inadequate the theories of heat proposed by Clausius and James Clark Maxwell, that are based on linear atomic motion. It was only in 1869 that Rankine admitted the success of these rival theories. He used his own theories to develop a number of practical results and to elucidate their physical principles. Interesting is his contribution on the study of shock waves are important

## REFERENCES

- BATCHELOR, G. K. 1993 *The theory of homogeneous turbulence*. Cambridge University Press, London.
- BATCHELOR, G. K. 1994 *An Introduction to Fluid Dynamics*. Cambridge University Press, London, New York, Melbourne.
- BERTATO, M., GIAIOTTI, D. B., MANZATO, A. & STEL, F. 2003 An interesting case of tornado in friuli-northeastern italy. *Atmospheric Research* **7–68**, 3–21.
- BLUESTEIN, H. B., LEE, W., BELL, M., WEISS, C. C. & PAZMANY, A. L. 2003 Mobile doppler radar observations of a tornado in a supercell near bassett, nebraska, on 5 june 1999. part ii: Tornado-vortex structure. *Mon. Wea. Rev.* **131**, 2968–2984.
- BLUESTEIN, H. B. & WEISS, C. C. 2004 Doppler radar observations of dust devils in texas. *Mon. Wea. Rev.* **132**, 209–224.
- BROWN, R. A., FLIKINGER, B. A., FORREN, E., SCHULTZ, D. M., SIRMANS, D., SPENCER, P. L., WOOD, V. T. & ZIEGLER, C. L. 2005 Improved detection of severe storms using experimental fine-resolution wrs-88d measurements. *Wea. Forecasting* **20**, 3–14.
- CRISCIANI, F. 2005 Lecture notes on Geophysical Fluid Dynamics - PhD course on Environmental Fluid Mechanics - ICTP/University od Trieste.
- DUTTON, J. A. 1995 *Dynamics of the Atmosphere motion*, chap. 7. Meteorological equations of motion. Dover Publication Inc., New York.
- FOGIEL, M. 2001 *Handbook of Mathematical, Scientific and Engineering formulas, tables, functions, graphs, transforms*. Reesearch & Education Association.
- GIAIOTTI, D. B. & STEL, F. 2005 The natural coordinate system and its applications in atmospheric physics - PhD course on Environmental Fluid Mechanics - ICTP/University od Trieste.
- GILL, A. E. 1982 *Atmosphere - Ocean Dynamics*, chap. 4.10, p. 84. Academic Press, London.
- HOLTON, J. R. 1972a *An Introduction to Dynamic Meteorology*, 3rd edn., chap. 2.2 The vectorial form of the momentum equation in rotating coordinates. Academic Press, San Diego, CA.
- HOLTON, J. R. 1972b *An Introduction to Dynamic Meteorology*, 3rd edn. Academic Press, San Diego, CA.
- PEDLOSKY, J. 1987 *Geophysical Fluid Dynamics*. Springer-Verlag, New York.